15

Design of Compact Planar Ultra-Wideband Bandpass Filters

Yasushi Horii
Kansai University
Japan

1. Introduction

Since the Federal Communication Commission (FCC) adopted a First Report and Order in 2002, a wide frequency range from 3.1 GHz to 10.6 GHz has been released for the marketing and operation of new types of wireless communication systems incorporating ultra-wideband (UWB) technology. Because of the high-speed data handling capability, the UWB system is expected to be used for delivering real-time HDTV video streaming, transmitting of non-compressible audio/visual signals, and replacing USB cables with wireless connections. In addition, due to the low-power consumption, new short-range wireless applications have attracted considerable attentions in the fields of home electronics, home entertainment, security sensors, and health care devices. To meet today's huge demands, the research on UWB devices has been greatly accelerated.

One of the difficulties in developing the UWB system is the bandwidth utilized for communication. Since the system uses very short impulse signals to transmit bit-data trains, it inherently requires an extremely wide frequency range. This unique feature always presses us to develop new technologies. In an RF front-end design, for instance, high-performance bandpass filters and antennas have been too large when we engaged in the conventional design methodology. An initial UWB filter was realized by a combination of low-pass and high-pass filters. Since then, tremendous efforts have been devoted to this subject, and a way to use a multi-mode resonator (MMR) was proposed in 2005. In this design, the first three resonant frequencies of the MMR are placed equally within the UWB band so as to create the huge passband response. By applying this technology, overall filter dimension was drastically reduced to less than 10 mm x 15 mm. After that, a variety of UWB filters have been proposed based on the MMR configuration. For example, some had a ground defected structure (DGS) or a periodic band gap (PBG) structure, and some used plural stages of MMRs to obtain the high selectivity performance. However, such approaches can sometimes cause an increase of the filter dimensions, leading to fabrication difficulties in a practical system design. Again, it should be noted that the short-range UWB systems are extremely low-power consumption and need to be pocket-sized or smaller.

My goal is to develop a super-compact planar UWB filter based on the microstrip line configuration. For this purpose, the following requirements are assumed;

(1) For frequency response

- To meet the FCC spectrum musk regulation
- Low insertion loss (less than 0.5 dB)
- Low ripples (less than 0.5 dB)
- Mild group delay variation (less than 0.2 ns)
- Transmission zeros above and below the passband

(2) For configuration

- Super-compact design (less than 5.0 mm x 5.0 mm)
- To use a microstrip line configuration
- No defections on a ground plane
- Compatible with the conventional PCB technology
- Low cost and mass productivity

In Sec. 2, a useful equivalent circuit is developed for design of super-compact UWB bandpass filters. In Sec. 3, actual filter designs are presented together with convenient design procedure to optimize the filter response.

2. Equivalent circuits

UWB bandpass filters need to be designed in an extremely wide frequency range from DC to around 20 GHz to meet the FCC spectrum musk regulation. The free-space wavelength at both passband edges are 96.8 mm at 3.1 GHz and 28.3 mm at 10.6 GHz. The wavelength will be compressed much more when a high permittivity substrate is applied to the filter. Therefore, even a small metal patch with 5 mm length can easily act as a resonator. This indicates that the UWB filters having a few millimeter dimension, work as a concentrated constant circuit at the lower frequency and as a distributed constant circuit at the higher frequency. Therefore, when the filter is designed, we should take these effects into consideration.

An equivalent circuit of the UWB bandpass filter, which is demonstrated in this chapter, is shown in Fig. 1. The notations, CL1, CL2, CL3 and CL4 in the figure, represent a coupled-line, each of which consists of tightly coupled three transmission lines placed in parallel with a small spacing. Among the coupled lines, a center line is short-circuited (SC) for grounding and the lines on both sides are open-circuited (OC) at their top, while these lines are connected to each other at their bottom. The coupled-line on the left-hand side (CL1 and CL2) is also coupled to that on the right-hand side (CL3 and CL4) with a coupling capacitance C_0. In addition, a coupled-inductor (CI) with a self-inductance L_0 and a mutual-inductance M_0 is presented in parallel with the capacitor C_0.

The typical circuit parameters of the filter are assumed as shown in Table 1, and the corresponding filter response is calculated by using the commercial circuit simulator ANSOFT Designer SV2. The result, presented in Fig. 2, shows that the filter has a huge flat passband together with deep transmission zeros just below and above the passband. In addition, well-suppressed out-of-passbands are obtained in a wide frequency range.

This UWB response can be explained by looking at the circuit from two points of view; one way is to look at the circuit as a *concentrated constant circuit*, which is available at the lower frequency, while the other way is to look at it as a *distributed constant circuit* in the higher frequency. According to such points of view, the equivalent circuits can also be expressed in a different way as shown in Fig. 3 and Fig. 5, respectively.

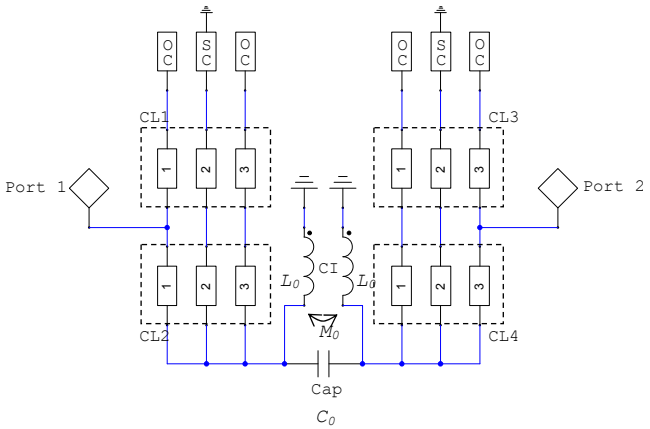

Fig. 1. An basic equivalent circuit of the super-compact planar UWB bandpass filters studied in this chapter. The circuit is configured by some lumped elements and distributed constant lines.

Coupled-lines	CL1	CL2	CL3	CL4
length	2.90 mm	1.60 mm	2.90 mm	1.60 mm
line width 1	0.50 mm	0.50 mm	0.50 mm	0.50 mm
spacing	0.35 mm	0.35 mm	0.35 mm	0.35 mm
line width 2	0.30 mm	0.30 mm	0.30 mm	0.30 mm
spacing	0.35 mm	0.35 mm	0.35 mm	0.35 mm
line width 3	0.50 mm	0.50 mm	0.50 mm	0.50 mm

Open circuit (OC)		Short circuit (SC)	
line width	0.50 mm	line width	0.30 mm
line length	0.00 mm	line length	0.50 mm

Coupled-inductor (CL)		Substrate	
self-inductance L_0	7.0 nH	thickness	0.80 mm
Mutual-inductance M_0	3.5 nH	relative permittivity	2.62
Capacitance C_0	0.70 pF		

Table 1. Circuit parameters of the equivalent circuit shown in Figs. 1, 3, and 5. Scattering characteristics of these circuits are presented in Fig. 2, 4, and 6. These parameters are tuned so as to obtain the UWB response.

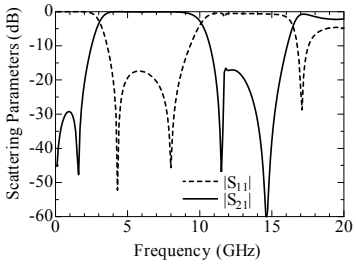

Fig. 2. Scattering characteristic of a UWB bandpass filter, calculated by an equivalent circuit shown in Fig. 1. Circuit parameters are listed in Table 1.

Fig. 3a, derived partially from the original equivalent circuit in Fig. 1, presents the circuit which creates the lower frequency response. The coupled-inductance (L_0, L_0 and M_0) inserted at the center of the figure can be transformed into three inductors (L_1, L_2 and L_3) as shown Fig. 3b, and a new series inductor L_2 forms an LC-tank circuit with the original series capacitor C_0. As a result, corresponding to the resonance of the LC-tank, a transmission zero is created below the passband. In addition, two shunt inductors (L_1 and L_3) and a series capacitor (C_0) stop the DC and the lower frequency signals from passing through the circuit.
Contrarily, the circuit components related to create the higher frequency response are derived from the original circuit in the same manner. The resultant equivalent circuit and its scattering characteristic are shown in Figs. 5 and 6, respectively. The length of the coupled-lines are chosen so that the open-circuited lines in the coupled-line work as a quoter-wavelength open-stub in a frequency range from 11 GHz to 15 GHz. Consequently, two stopbands are created above 11 GHz in accordance with the lines.
This study clearly indicates that the lower and the higher frequency responses in Fig. 2 are produced by the combination of the concentrated constant circuit and the distributed constant circuit, and each response can be controlled independently by tuning corresponding circuit parameters. In other words, the lower and the higher cutoff frequencies of the passband are created by different mechanisms. Thus, the equivalent circuit presented in Fig. 1 gives us a great insight of a new filter topology.

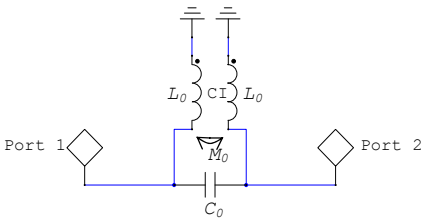

(a)

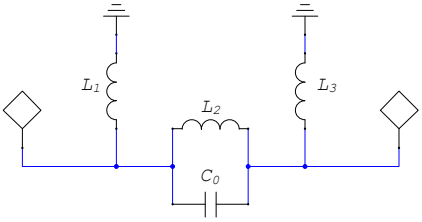

(b)

Fig. 3. An equivalent circuit, describing the lower frequency response of the UWB filter. (a) The circuit configured by lumped elements, which is derived from the original equivalent circuit presented in Fig. 1. (b) The coupled-inductor in Fig. 3a can be transformed equivalently into three inductors. An LC-tank creates a transmission zero below the UWB passband.

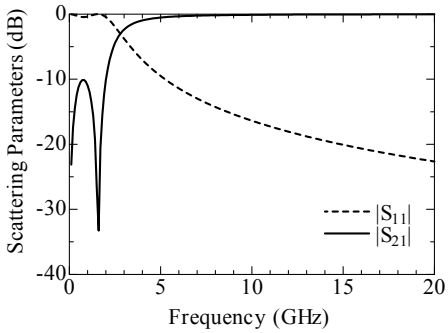

Fig. 4. Scattering characteristic of the equivalent circuit shown in Fig. 3a with circuit parameters listed in Table 1.

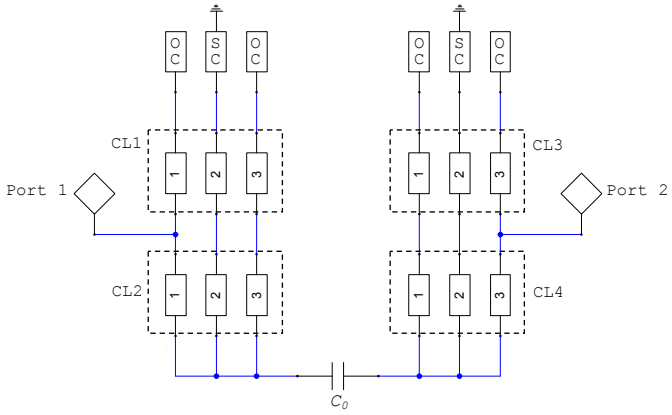

Fig. 5. An equivalent circuit, describing the higher frequency response of the UWB filter. The circuit is mainly composed of distributed constant transmission lines, which work as a quoter-wavelength open-stub to create a stopband above the UWB passband.

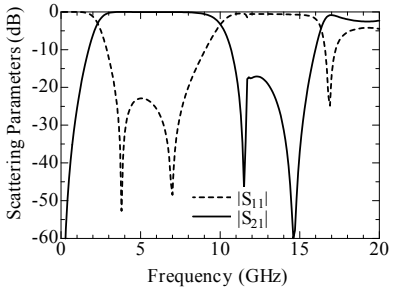

Fig. 6. Scattering characteristic of the equivalent circuit shown in Fig. 5 with circuit parameters listed in Table 1.

3. Planar UWB bandpass filters

3.1 UWB bandpass filters with tightly coupled E-shaped electrodes

Fig. 7 shows a circuit layout of a planar-type UWB bandpass filter designed in accordance with the equivalent circuit presented in Fig 1. All the circuit elements, designed using microstrip line configuration, are fabricated on a dielectric substrate with thickness H_{SUB} and relative permittivity ε_r. The coupled-lines in Fig. 1, CL1-CL2 and CL3-CL4, are created by tightly coupled three transmission lines. Length and width of the lines are designated by (L_1, W_1), (L_2, W_2), (L_3, W_3), (L_4, W_4), (L_5, W_5), and (L_6, W_6) starting from the leftmost line. The spacing between the lines in the coupled-line is shown by S. The thin line with width W_B is given to the bottom of each coupled-line to connect them together. The lines on both sides in the coupled-line are open-circuited at their top, while the center line is short-circuited for grounding. Because the shape of the coupled-line resembles to the letter "E", the coupled-line is called an "E-shaped electrode". The input and output microstrip lines with width W_{MSL} are connected to the leftmost and rightmost lines with a small offset D from the bottom of the electrode. By applying such an architecture, the distributed constant circuit presented in Fig. 5 is composed.

Next, we need to consider how to create the concentrated constant circuit parameters in the actual model. If the circuit layout was develped as a precise copy of the equivalent circuit, the overall filter dimension would be large. For significant size reduction, the function of the concentrated constant circuit should be realized by utilizing the architecture of the distributed constant circuit. Fortunately, the series capacitance C_0 is yielded by placing two E-shaped electrodes very closely with a small gap G. In addition, it is also expected that two short-circuited lines in the electrodes yield a required self-inductance L_0 and a mutual-inductance M_0 by a magnetic coupling between them. Thus, the required concentrated circuit behaviour observed at the lower frequency can be created by fine-tuning of the filter layout of the distributed constant circuit. These structural parameters, summarized in Table 2, were determined by using a full-wave EM-simulator Ansoft HFSS based on the finite element method. Design methodology is introduced in the latter subsection 3.4.

Fig. 8 presents the frequency dependence of the transmission coefficient $|S_{21}|$ and the reflection coefficient $|S_{11}|$. It can be read from the figure that the filter has a very wide passband from 3.8 GHz to 10.4 GHz (-3 dB criteria), which corresponds to the relative bandwidth of 93.6 %. The minimum insertion loss in the passband is about 0.16 dB at 9.5 GHz, and ripples are less than 0.5 dB from 5.3 GHz to 10.0 GHz. Furthermore, the $|S_{11}|$ is less than -10 dB from 5.1 GHz to 10.0 GHz. In addition, this filter has attenuation poles at 1.5 GHz and 11.3 GHz, and two reflection poles at 7.3 GHz and 9.5 GHz. The location of these poles is deeply related to the selectivity of the passband and the group delay of the filter.

Fig. 9 shows a photograph of the prototype model fabricated on a Rexolite 2200 substrate with a relative permittivity of 2.62 and a thickness of 0.8 mm. A circuit board plotter LPKF Protomat C30s was used to cut the metallization on the substrate along the contour of the electrodes and microstrip lines, and then unnecessary metallizations were removed by hand. To create an input and an output ports, two SMA connectors were soldered to the microstrip lines. Outer dimension of the prototype model was 10 mm x 15 mm x 0.8 mm.

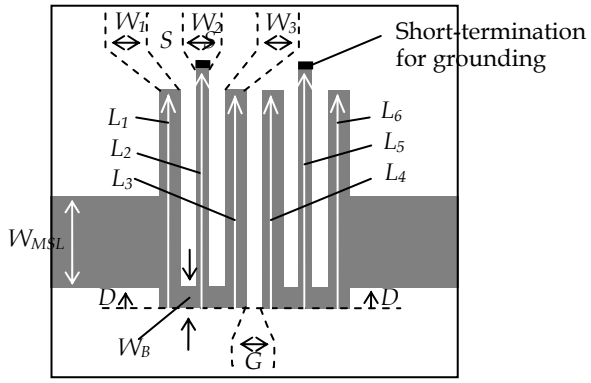

Fig. 7. A circuit layout of the planer UWB bandpass filter with tightly coupled E-shaped electrodes. Structural parameters are listed in Table 2.

Coupled-lines							
L_1	L_2	L_3	L_4	L_5	L_6	*Spacing bw lines*	*Spacing bw ELs**
5.0	5.5	5.0	5.0	5.5	5.0		
W_1	W_2	W_3	W_4	W_5	W_6	S	G
0.5	0.3	0.5	0.5	0.3	0.5	0.35	0.05

	I/O microstip lines			Substrate	
W_B	D	W_{MSL}	Z_0	H_{SUB}	ε_r
0.5	0.5	2.0	50 ohm	0.8	2.62

Table 2. Structural parameters of the planar UWB bandpass filter with tightly coupled E-shaped electrodes shown in Fig. 7. Unit for dimensional parameters is in *mm*.

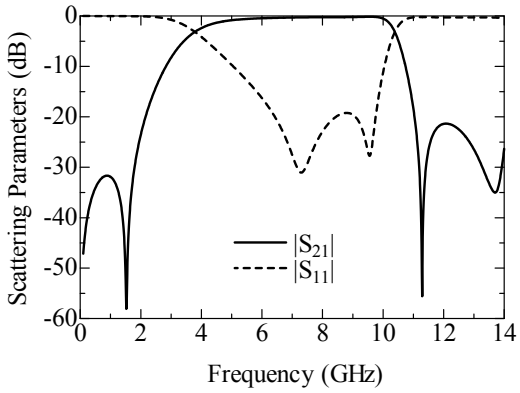

Fig. 8. Simulated scattering characteristic of the planar UWB bandpass filter with tightly coupled E-shaped electrodes shown in Fig. 7 with circuit parameters listed in Table 2.

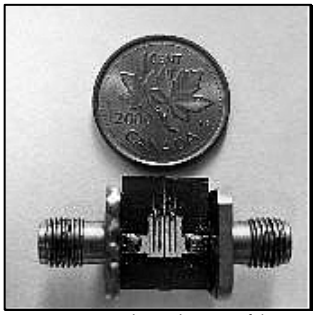

Fig. 9. A prototype of the planar UWB bandpass filter with tightly coupled E-shaped electrodes, illustrated in Fig. 7 with circuit parameters listed in Table 2. The filter is fabricated on a Rexolite 2200 substrate with a relative permittivity of 2.62 and a thickness of 0.8 mm.

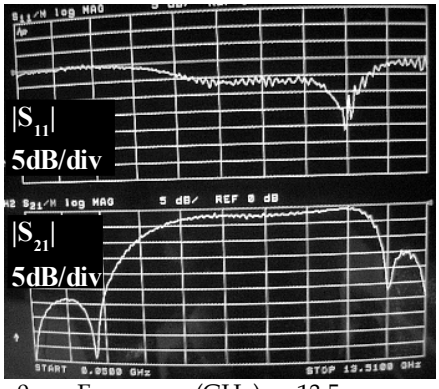

(a)

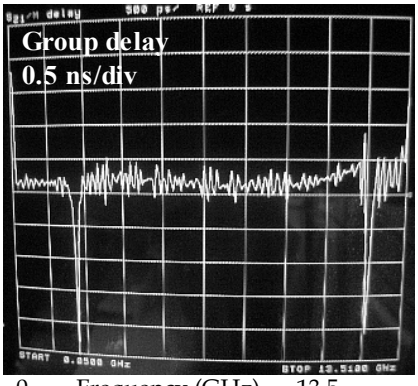

(b)

Fig. 10. Measured scattering characteristics of the planar UWB bandpass filter with tightly coupled E-shaped electrodes. (a) The reflection coefficient $|S_{11}|$ (top) and the transmission coefficient $|S_{21}|$ (bottom). Unit in vertical axis is 5 dB/div. (b) Group delay. Unit is 0.5 ns/div.

Fig. 10a shows a magnitude of the scattering coefficients $|S_{11}|$ and $|S_{21}|$ of the filter. It can be read from the curve $|S_{21}|$ that the wide passband from 5.0 GHz to 11.3 GHz and deep attenuation poles at 2.3 GHz and 12.2 GHz are obtained. Although the passband is a little bit higher than the theory due to too much milling of the substrate in the pattern making process, the shape of the measured $|S_{21}|$ shows good agreement with the theory as a whole. The minimum insertion loss of less than 0.8 dB is attained at 10.8 GHz. In general, the insertion loss is caused by conductor loss, dielectric loss and radiation loss. However, the insertion loss of the passband is mainly caused by the wider gap than the initial design, leading to a weakened coupling between the E-shaped electrodes.

Fig. 10b presents a group delay measured between SMA connectors. The result includes small vibrations because the network analyzer used for this measurement was quite old and it lacked stability. However, the real group delay can be estimated by reading the average

value from the measured result. The variation of the group delay is estimated around 0.2 ns in the passband and it gets slightly higher at up to 0.4 ns at the higher edge of the passband. A mild group delay is quite useful to convey the short pulse signal from the input to the output without serious distortion.

For size reduction of the filter, using the higher dielectric permittivity substrate is the well-known standard approach. As for the design examples, two filters fabricated on the substrate with ε_r=5 or ε_r=10 are designed with the structural parameters summarized in Tables 3. The simulated scattering characteristics for these models are shown in Fig. 11. Though the dielectric and conductor losses are not included in the simulation, it can be confirmed that these filters have a flat UWB passband with the reflection coefficient of less than -15 dB. In addition, compared with the conventional UWB filters engaged in multiple-mode resonators, significant size reduction is attained.

Coupled-lines							
L_1	L_2	L_3	L_4	L_5	L_6	*Spacing bw lines*	*Spacing bw ELs**
3.7	3.7	3.7	3.7	3.7	3.7		
W_1	W_2	W_3	W_4	W_5	W_6	S	G
0.3	0.3	0.3	0.3	0.3	0.3	0.35	0.01
Input / Output microstrip lines				Substrate			
	I/O microstip lines			Substrate			
W_B	D	W_{MSL}	Z_0	H_{SUB}	ε_r		
0.3		0.83	50 ohm	0.5	5.0		

(a) * between Electrodes

Coupled-lines							
L_1	L_2	L_3	L_4	L_5	L_6	*Spacing bw lines*	*Spacing bw ELs**
2.7	2.7	2.7	2.7	2.7	2.7		
W_1	W_2	W_3	W_4	W_5	W_6	S	G
0.2	0.2	0.2	0.2	0.2	0.2	0.2	0.008
Input / Output microstrip lines				Substrate			
	I/O microstip lines			Substrate			
W_B	D	W_{MSL}	Z_0	H_{SUB}	ε_r		
0.2		0.44	50 ohm	0.5	10.0		

(b) * between Electrodes

Table 3. Structural parameters of the miniaturized UWB bandpass filter with tightly coupled E-shaped electrodes fabricated on the higher permittivity substrate. (a) Substrate with ε_r=5 is used. (b) Substrate with ε_r=10 is used.

The total area of the filter body (area of the E-shaped electrodes and the gap between them) is 3.21 mm x 3.7 mm x 0.5 mm for ε_r=5 model and 2.008 mm x 2.7 mm x 0.5 mm for ε_r=10 model, respectively.

Contrary to the super-compactness, it should be noted that the filters fabricated on the higher permittivity substrate always require an extremely small gap between the electrodes in order to create the necessary series capacitance C_0. For instance, when the substrate with ε_r=10 is used, the gap width of 0.008 mm is required. However, 0.05 mm gap is the recent

fabrication limit for the standard PCB technology. If the narrower gap needs to be fabricated, the high-cost laser-based process would be indispensable for structuring the circuit.

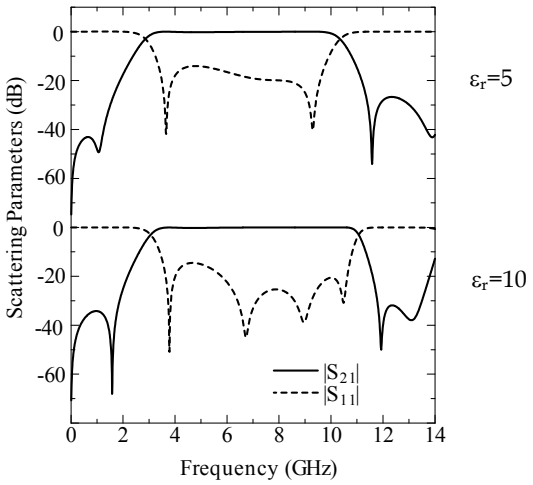

Fig. 11. Simulated scattering characteristics of the miniaturized UWB bandpass filter with tightly coupled E-shaped electrodes. Filters are fabricated on the high permittivity substrate with ε_r=5 (top) or ε_r=10 (bottom). Structural parameters are summarized in Tables 3a and 3b, respectively.

3.2 UWB bandpass filters with capacitor-loaded E-shaped electrodes

The model introduced in the former subsection would be useful if the small gap between the E-shaped electrodes could be fabricated accurately using the conventional PCB technology. However, as mentioned above, when we design the smaller filter using the higher permittivity substrate, the gap width will be significantly narrower.

The easier way to reduce such fabrication difficulties is to introduce a chip capacitor onto the gap to compensate for the insufficient gap capacitance. A circuit layout of a new planer UWB bandpass filter with capacitor-loaded E-shaped electrodes is shown in Fig. 12. The small chip capacitor with capacitance C_P is loaded between the E-shaped electrodes with an offset P from the bottom of the electrodes.

To begin with, the relation between the gap width G and the transmission coefficient $|S_{21}|$ is shown in Fig. 13a when the chip capacitor is not yet installed on the gap. Except for the value of the gap width G, structural parameters are the same as the model shown in Fig. 7. Apparently, when the gap becomes wider, the passband response is significantly damaged and reduced. To study the usefulness of the chip capacitor, let's start the filter design with G=0.3 mm.

Fig. 13b presents the $|S_{21}|$ when the chip capacitance C_P is varied from 0.0 pF (without a capacitor) to 2.0 pF. The capacitor is assumed to be fabricated at the bottom of the electrodes (P=0.0 mm), and the gap width is fixed as G=0.3 mm. In this structure, the required series capacitance C_0 is mostly supplied by the chip capacitor C_P. It is confirmed from the graph

that the response around 3 GHz is improved drastically by choosing an appropriate capacitance C_P. In this study, when C_P is 0.5 pF, the flatter passband response is obtained.
In addition, the stopband response at the higher frequency above the passband is also important. The offset of the chip capacitor P is related to the position of the transmission zeros in the higher frequency region, because the effective length of the third and forth lines of the electrodes, which work as an open-stub band elimination filter, are varied by changing the chip offset P. Fig 13c shows the simulated $|S_{21}|$ when the P is varied from 0.0 mm to 1.5 mm. Calculation is carried out for the fixed gap width G=0.3 mm and the chip capacitance C_P=0.5 pF. It can be read from the graph that the transmission zero obtained above the passband shifts slightly higher with the increase of P, and a pulse-like response around 13 GHz disappears from there. As a result, the insertion loss of more than 30 dB is attained above 11.5 GHz by choosing as P=1.5 mm. According to these theoretical considerations, the structural parameters of the final model are derived as listed in Table 4.

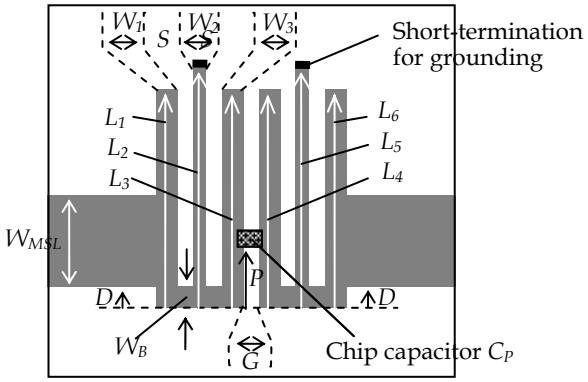

Fig. 12. A circuit layout of a planer UWB bandpass filter with capacitor-loaded E-shaped electrodes. Structural parameters are listed in Table 4.

As shown in Fig. 14, a prototype model with structural parameters listed in Table 4, is fabricated to confirm the theoretical predictions. As the chip capacitor, a high frequency multi-layered ceramic capacitor VK105 from TAIYO YUDEN was used and soldered between the electrodes with the offset P=1.5 mm.
For comparison, two types of filters are demonstrated; one is the filter before installing the chip capacitor (corresponding to the top graph in Fig. 15a), and the other is the filter after installing the chip capacitor (corresponding to the bottom graph in Fig. 15a). As predicted by the simulation in Fig.13a, the measured transmission coefficient $|S_{21}|$ is badly damaged due to the shortage of the series capacitance. However, by supplying the additional capacitance with C_P=0.5 pF, an extremely wide and flat passband is created from 3.1 GHz to 11.4 GHz, corresponding to the fractional bandwidth of 114 %. The return loss of more than 10 dB is attained from 3.7 GHz to 11.0 GHz. Furthermore, as shown in Fig. 15b, the measured group delay of the filter is quite mild, and the in-band group delay variation is less than 0.2 ns. Thus, the filter response is improved quite easily and drastically by supplying the small chip capacitor onto the gap.

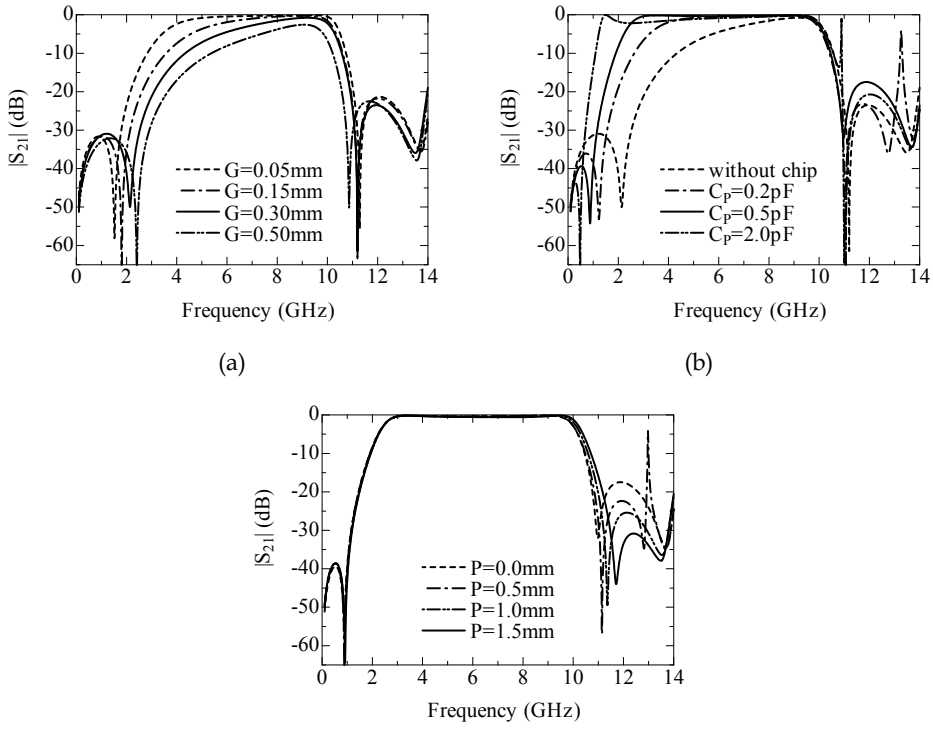

Fig. 13. Calculated transmission coefficients $|S_{21}|$ of the planer UWB bandpass filter with capacitor-loaded E-shaped electrodes shown in Fig. 12. Design starts with the initial parameters listed in Table 2. (a) The effect of the gap width G when the chip capacitor is not installed. (b) The effect of the chip capacitor C_P, when G=0.3 mm and P=0.0 mm are assummed. (c) Tuning of the higher frequency response by changing the chip offset P. The parameters G=0.3 mm and C_P=0.5 pF are assummed.

Coupled-lines							
L_1	L_2	L_3	L_4	L_5	L_6	*Spacing bw lines*	*Spacing bw ELs**
5.0	5.5	5.0	5.0	5.5	5.0		
W_1	W_2	W_3	W_4	W_5	W_6	S	G
0.5	0.3	0.5	0.5	0.3	0.5	0.35	0.3
	I/O microstrip lines			Substrate		Chip capacitor	
W_B	D	W_{MSL}	Z_0	H_{SUB}	ε_r	C_P	P
0.5	0.5	2.0	50 ohm	0.8	2.62	0.5 pF	1.5

* between Electrodes

Table 4. Structural parameters of the planer UWB bandpass filter with capacitor-loaded E-shaped electrodes shown in Fig. 12. Unit for dimensional parameters is in *mm*.

Fig. 14 A prototype of the UWB bandpass filter with capacitor-loaded E-shaped electrodes, shown in Fig. 12 with circuit parameters listed in Table 4. The filter is fabricated on a Rexolite 2200 substrate with a relative permittivity of 2.62 and a thickness of 0.8 mm. A 0.5 pF chip capacitor is loaded between the electrodes.

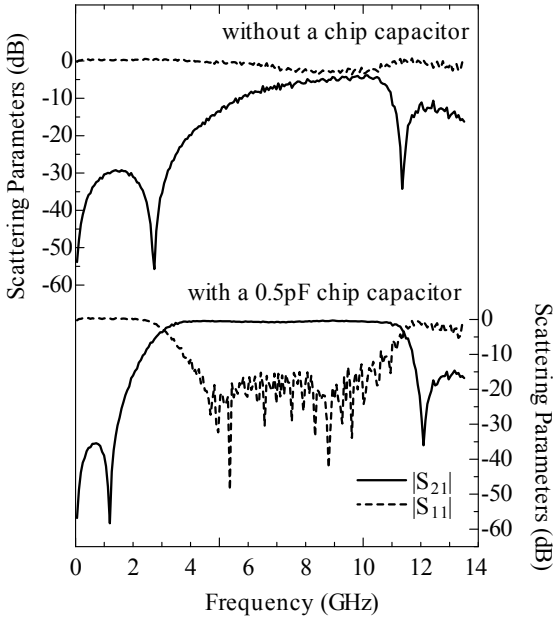

(a)

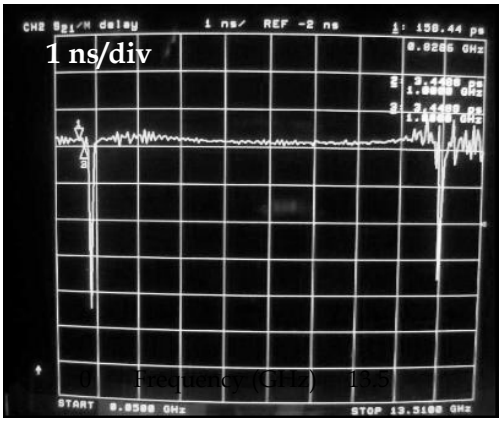

(b)

Fig. 15. Measured scattering characteristics of the UWB bandpass filter with capacitor-loaded E-shaped electrodes. (a) The reflection coefficient $|S_{11}|$ and the transmission coefficient $|S_{21}|$ of the filters without a chip capacitor (top half of the graph) and with a 0.5 pF chip capacitor (bottom half of the graph). Basic structural parameters are listed in Table 5. (b) The group delay between SMA connectors. Unit is 1 ns/div.

3.3 Asymmetric UWB bandpass filters with improved out-of-passband response

The UWB bandpass filters with tightly-coupled or capacitor-loaded E-shaped electrodes were both attractive in respects to the compactness, low-cost fabrication, and mass-productivity. In addition, the superior passband selectivity was realized by creating the transmission zeros just below and above the passband. However, the FCC specification also requires a high rejection level in the stopband. In order to improve the stopband response, an asymmetric UWB bandpass filter with capacitor-loaded E-shaped electrodes was newly developed. This technology is introduced in this subsection.

As mentioned above, the transmission zeros above the passband are created by the quarter-wavelength open-stubs in the electrodes. This means that the stopband response can be improved by tuning the length of the stubs so that the transmission zeros are located at regular intervals in the stopband region. This fine-tuning process can be done simply by using an optimizer installed in the commercial EM simulators, or by changing the length of the stubs manually.

In the actual design, the fine-tuning process, started with the symmetric UWB bandpass filter with capacitor-loaded E-shaped electrodes presented in Fig. 12. Since the lines in the electrodes couple to each other, this process will be time-consuming and tedious if the optimization is done manually.

Fig. 16 shows the circuit layout of the optimized asymmetric bandpass filter, the structural parameters of which are summarized in Table 5. For comparison, the simulated scattering characteristics are shown in Fig. 17, together with the original symmetric filter shown in Fig. 12 with the structural parameters given in Table 4. The optimized asymmetric bandpass filter has the wide stopband from 11.5 GHz to 18.5 GHz with the rejection level of more than 10 dB, while the original flat and wide passband response is maintained.

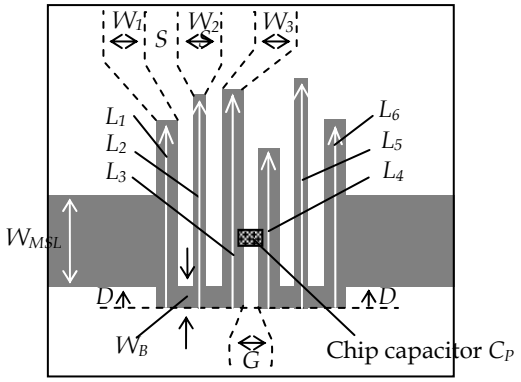

Fig. 16. A circuit layout of the asymmetric UWB bandpass filter with capacitor-loaded E-shaped electrodes. Structural parameters are listed in Table 6 and FEM-simulated scattering characteristics are presented in Fig. 17.

Coupled-lines							
L_1	L_2	L_3	L_4	L_5	L_6	*Spacing bw lines*	*Spacing bw ELs**
4.5	4.8	4.9	3.7	5.1	4.2		
W_1	W_2	W_3	W_4	W_5	W_6	S	G
0.5	0.3	0.5	0.5	0.3	0.5	0.3	0.5
	I/O microstrip lines			Substrate		Chip capacitor	
W_B	D	W_{MSL}	Z_0	H_{SUB}	ε_r	C_P	P
0.5	0.5	2.0	50 ohm	0.8	2.62	0.5	1.0

* between Electrodes

Table 5. Structural parameters of the asymmetric UWB bandpass filter with capacitor-loaded E-shaped electrodes shown in Fig. 16. Unit for dimensional parameters is in *mm*.

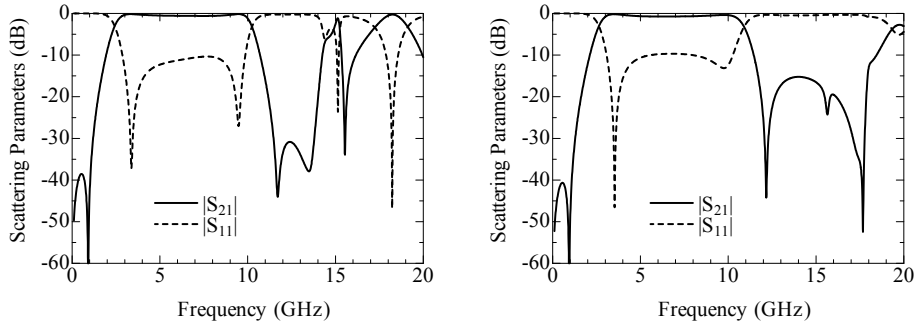

(a) (b)

Fig. 17. FEM-simulated scattering characteristics. (a) The symmetric UWB bandpass filter with capacitor-loaded E-shaped electrodes (original model). (b) The asymmetric UWB bandpass filter with capacitor-loaded E-shaped electrodes (optimized model).

3.4 Design procedure of UWB bandpass filters

Different from other UWB bandpass filters proposed so far, the couplings between the filter components play an important role in this filter to obtain a superior UWB response in a limited filter dimension. For example, the filter uses the electric coupling between the electrodes, the electric coupling between the thin lines of the electrodes, and the magnetic coupling between the short-circuited stubs of the electrodes. However, this makes it difficult to use the conventional filter theory for this kind of filter design. Instead, the filter can be designed easily in accordance with a simple design procedure as follows;

1) The length of the open-stubs in each E-shaped electrodes (L_1, L_3, L_4, and L_6) needs to be chosen as a quarter-wavelength so as to obtain some transmission zeros above the UWB passband. This process is usually done under L_1=L_3=L_4=L_6. The higher cutoff frequency is roughly determined by this.
2) The length of the short-stubs in each electrode (L_2 and L_5) needs to be chosen so as to obtain a transmission zero below the UWB passband. The lower cutoff frequency is roughly given by this step.
3) The coupling between the E-shaped electrodes should be tuned by changing the gap width between the electrodes, G, so as to create a flat UWB passband. It should be noted that the larger gap can easily damege the response at the lower edge of the passband.
4) If a chip capacitor with an appropriate capacitance is loaded between the gap, the fabrication difficulty will be reduced significantly.
5) Fine-tuning of other structural parameters are needed to obtain the better filter response. The center frequency of the UWB passband can be adjusted in some extent by the width of the line W_B at the bottom of the E-shaped electrode. The in-band ripples in the transmission coefficient can be reduced in this process.
6) The higher stopband response can be improved slightly by giving an appropriate offset D to the input and output microstrip lines connecting to the electrodes.

By this, an excellent UWB passband will be attained. To create the better stopband response, fine-tuning of the open-/short-stubs in the electrodes is quite useful as demonstrated in the former discussion.

7) To create the better stopband, the line length in the electrodes should be tuned independently by using an optimizer installed in the commercial EM simulators or by changing the length manually.

According to these instructions, all the filters presented in this chapter were designed.

4. Conclusions

In this chapter, three types of compact UWB bandpass filters with plural transmission zeros below and above the passband are introduced together with the useful design procedure. Compared with other conventional filters, the proposed filter can be made drastically small in size with the help of a tiny chip capacitor. In addition, the circuit pattern of the filter is given only at the top of the substrate and a perfect ground plane is remained without any

defections. This will be a great advantage when the filter is fabricated on a double-layered substrate. Furthermore, the microstrip-line-based filter patterns can be printed out together with other circuit petterns at the same time using the common PCB process. Thus, the proposed filters have tremendous attractive features in the engineering of the latest UWB technology, in respects to the super-compactness, easy fabrication, excellent compatibility to other circuits, low-cost and mass productivity.

5. References

Federal Communications Commission (2002), "Revision of Part 15 of the Commission's Rules Regarding UWB Transmission Systems, First report and order", *Federal Communication Commissions (FCC)*, 02.V48.

Ishida, H. & Araki, K. (2004) "Design and analysis of UWB bandpass filter with ring filter", *IEEE International Microwave Symp.*, Proceedings.

Zhu, L.; Sun S. & Menzel W. (2005), "Ultra-wideband (UWB) bandpass filters using multiple-mode resonator", *IEEE Microwave Wireless Compon. Lett.*, vol.15, no.11, pp.796-798.

Horii, Y. (2007). "A compact planar ultra-wideband bandpass filter composed of coupled E-shaped electrodes", *European Microwave Conf.*, Proceedings.

Horii, Y.; Ishikawa, K.; Kaneko, T. & Azuma, Y. (2007). "Development of design procedure for compact planar ultra-wideband (UWB) bandpass filters", *Asia-Pacific Microwave Conf.*, Proceedings.

Horii, Y. (2008). "Super-compact planar ultra-wideband (UWB) bandpass filter composed of capacitor-loaded E-shaped electrodes", *European Microwave Conf.*, Proceedings, pp.361-364.

Kaneko, T.; Azuma, Y.; Ishikawa, K. & Horii, Y. (2008). "Ultra-wideband (UWB) bandpass filter composed of asymmetric E-shaped electrodes for improved out-of-passband", *Asia-Pacific Microwave Conf.*, Proceedings.

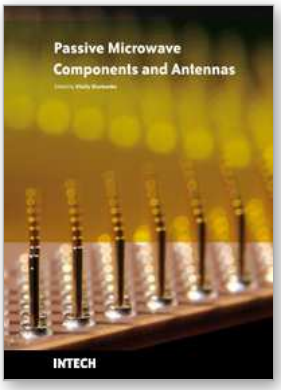

Passive Microwave Components and Antennas

Edited by Vitaliy Zhurbenko

ISBN 978-953-307-083-4
Hard cover, 556 pages
Publisher InTech
Published online 01, April, 2010
Published in print edition April, 2010

Modelling and computations in electromagnetics is a quite fast-growing research area. The recent interest in this field is caused by the increased demand for designing complex microwave components, modeling electromagnetic materials, and rapid increase in computational power for calculation of complex electromagnetic problems. The first part of this book is devoted to the advances in the analysis techniques such as method of moments, finite-difference time- domain method, boundary perturbation theory, Fourier analysis, mode-matching method, and analysis based on circuit theory. These techniques are considered with regard to several challenging technological applications such as those related to electrically large devices, scattering in layered structures, photonic crystals, and artificial materials. The second part of the book deals with waveguides, transmission lines and transitions. This includes microstrip lines (MSL), slot waveguides, substrate integrated waveguides (SIW), vertical transmission lines in multilayer media as well as MSL to SIW and MSL to slot line transitions.

InTech Europe
University Campus STeP Ri
Slavka Krautzeka 83/A
51000 Rijeka, Croatia
Phone: +385 (51) 770 447
Fax: +385 (51) 686 166
www.intechopen.com

InTech China
Unit 405, Office Block, Hotel Equatorial Shanghai
No.65, Yan An Road (West), Shanghai, 200040, China
中国上海市延安西路65号上海国际贵都大饭店办公楼405单元
Phone: +86-21-62489820
Fax: +86-21-62489821